15.5 WSR-88D DUAL POLARIZATION INITIAL OPERATIONAL CAPABILITIES

Michael J. Istok*
NOAA/National Weather Service, Office of Science and Technology, Silver Spring, MD

Mark Fresch
NOAA/National Weather Service, Office of Hydrologic Development, Silver Spring, MD

Zack Jing, Steven D. Smith, and Richard Murnan
NOAA/National Weather Service, Office of Operational Systems, Norman, OK

Alexander Ryzhkov, John Krause, and Michael Jain
NOAA/Oceanic and Atmospheric Research, National Severe Storms Laboratory, Norman, OK

Paul Schlatter and John Ferree
NOAA/NWS/Office of Climate, Water, and Weather Services, Norman, OK

Brian R. Klein and Dan Stein,
Wyle Information Systems, LLC., Silver Spring, MD

Gregory Cate
NOAA/National Weather Service, Office of Science and Technology, Norman, OK

Robert E. Saffle
Noblis, Inc., Falls Church, VA

1. INTRODUCTION

The Weather Surveillance Radar – 1988 Doppler (WSR-88D) tri-agencies (Departments of Commerce, Defense, and Transportation; DOC, DOD, DOT, respectively) have determined that adding dual polarization capability to the WSR-88D would provide mission benefits including improved hail detection for severe thunderstorm warnings, improved rainfall estimation for flood and flash flood warnings, rain/snow discrimination for winter weather warnings and advisories, data retrieval from areas of partial beam blockage to improve services in mountainous terrain, and removal of non-weather artifacts such as birds and ground clutter to improve overall data quality for algorithms and numerical model input.

Systems engineering for the dual polarization upgrade to the WSR-88D is well underway. System Specifications for the dual polarization upgrade were established, a contract was awarded in September 2007 to develop and deploy the Radar Data Acquisition (RDA) portion of the upgrade, and a Critical Design Review (CDR) was conducted in October 2008.

The National Oceanic and Atmospheric Administration (NOAA) National Weather Service's (NWS) Office of Science and Technology (OST) is leading a broad team of NOAA groups including the NWS's Office of Hydrologic Development (OHD); Office of Operational Systems (OOS) Radar Operations Center (ROC); Office of Climate, Water and Weather Services (OCWWS); and the Office of Atmospheric Research's (OAR's) National Severe Storms Laboratory (NSSL) to implement changes to the Radar Product Generator (RPG) to ingest, process and distribute the dual polarization data and derived products. The effort is focused on the initial operating capability (IOC) of the dual polarization upgrade and has included establishing algorithm, product, and display requirements; and developing, documenting, and implementing data preprocessing, algorithm, and product software. The IOC algorithms are based on prototype development at NSSL.

The NWS Advanced Weather Interactive Processing System (AWIPS) program has completed implementation of software changes to ingest, display, and manipulate the dual polarization products. These changes were completed in Operational Build (OB) 9 and therefore will be included in the initial release of AWIPS-2 (Henry et al., 2009). The OCWWS Warning Decision Training Branch is developing training plans and materials for NWS forecasters. WSR-88D Build 12 will contain the software change for dual polarization IOC. Formal system testing is scheduled to begin in October 2009, with field beta testing beginning in June 2010, and deployment beginning in October 2010.

This paper will describe the functional characteristics of the data generated by the dual polarization WSR-88D RDA, provide an overview of the RPG IOC algorithms and products, and present examples showing

* *Corresponding author address*: Michael J. Istok, NOAA/National Weather Service, W/OST32
1325 East West Highway, Silver Spring, MD, 20910
Email: Michael.Istok@noaa.gov

new capabilities implemented on AWIPS to support dual polarization operational use.

2. WSR-88D DUAL POLARIZATION BASE DATA CHARACTERISTICS

The WSR-88D will use the approach described in Doviak et al. (2000) of simultaneous transmission of horizontal and vertically polarized pulses to acquire dual polarization data. This approach minimizes dwell time for polarimetric variable computations and therefore will not lengthen volume scan update rates, but splitting the power results in a return signal with reduced sensitivity. The operational impact of this reduced sensitivity has been evaluated by subject-matter experts and WFO forecasters. Both scientific analysis and WFO usage reports indicated no significant operational impact due to the reduced sensitivity (Scharfenberg, Elmore, et al., 2005). Signal processing techniques are also being investigated to recover much of the reduced sensitivity (Ivic, 2008).

The WSR-88D RDA system controls antenna scanning and signal processing and formats base data radials which are transmitted to the RPG for algorithm processing and product generation. Three fields of dual polarization base data -- differential reflectivity, correlation coefficient, and differential phase -- will be added to moment data currently output by the RDA. Consistent with conventional moment data processing, dual polarization data will be provided at a range resolution of 250 meters(m) up to maximum range of 300 kilometers (km), and on the low elevation split cuts the radials will be provided to the RPG at a resolution of 0.5 degrees azimuth. The two other data enhancements introduced in WSR-88D Build 10 -- 250m range resolution for reflectivity data and 300km maximum range for Doppler moments -- will be extended to all the remaining elevations of the volume scan.

3. DUAL POLARIZATION ALGORITHMS AND PRODUCTS FOR THE WSR-88D RPG

3.1 *Algorithm Development and Evaluations*

Dual polarization radar is a unique instrument for classification of radar echoes. Having dual polarization capability is essential for discriminating between meteorological and non-meteorological scatterers and for distinguishing between different hydrometeor types, such as rain, hail, graupel, and snow of different types.

Principles of fuzzy logic form the basis for most hydrometeor classification algorithms. Using a prototype dual polarimetric WSR-88D, hydrometeor classification was tested in an operational environment in Oklahoma in 2002 – 2003 during a demonstration project called the Joint Polarization Experiment (JPOLE) (Ryzhkov et al. 2005a). Such a capability together with other polarization products was very well received by NWS forecasters during this operational demonstration (Scharfenberg et al. 2005). One of the first versions of the NSSL hydrometeor classification algorithm (HCA) demonstrated good skill to detect hail during JPOLE (Heinselman and Ryzhkov 2006).

The version of HCA which was accepted for operational implementation on the polarimetric WSR-88D is described in Park et al. (2009). This version contains several modifications and refinements of the early classification procedures. These modifications include the estimation of a data quality index that characterize possible impact of all error sources on radar measurements, the assignment of a matrix of weights which characterizes classification importance of each variable with respect to every class of radar echo, and implementation of class designation based on the distance from the radar and the parameters of the melting layer which are determined as functions of azimuth with polarimetric radar measurements.

The Melting Layer Detection Algorithm (MLDA) is an important part of HCA. The MLDA module developed at NSSL was tested on a variety of storms using an S-band radar in Oklahoma (Giangrande et al. 2008) and using a C-band radar in Ontario, Canada (Boodoo et al. 2008), and it has demonstrated robust performance in both climate regions.

Multiparameter measurements with polarimetric radar enable substantial improvement in the accuracy of radar rainfall estimation compared to single polarization radar. Earlier versions of polarimetric quantitative precipitation estimation (QPE) were validated during JPOLE using dense networks of the micronet and mesonet gages (Ryzhkov et al. 2005). It was shown that combining reflectivity, differential reflectivity, and specific differential phase in a so-called synthetic algorithm yields dramatic reduction in the errors of QPE at the distances below 100 km from the radar. Further studies indicated that it is crucial to combine HCA and QPE and make rainfall estimation contingent on the results of hydrometeor classification within the radar sample bin. This would especially help to better quantify precipitation at longer distances from the radar where the resolution volume might be filled with frozen or mixed-phase particles. This idea was implemented in a second version of the polarimetric QPE algorithm (QPE v2) which was validated using Oklahoma Mesonet gages for 43 rain events (Giangrande and Ryzhkov 2008). It was shown that utilizing the QPEv2 polarimetric algorithm instead of the single polarization method results in a reduction of the bias and root-mean-square (RMS) error of hourly rainfall estimates up to 200 km from the radar. At close distances the RMS error is reduced by roughly a factor of 2. This second version will be included in the IOC. A complementary study (Kitzmiller et. al. 2007) showed that the polarimetric algorithm yielded RMS errors equivalent to those of single-polarization radar estimates after mean-field bias correction with observations from a dense rain gauge network.

3.2 *Algorithm Requirements Capture and Validation Approach*

Over the years, NSSL researchers and software designers have developed several dual polarization algorithms that are in different stages of maturity.

Those mature algorithms that have a proven capability to yield meteorological benefits will be the first algorithms deployed. By nature, research software incorporates many changes through the years and in some cases only a select few truly understand the logic within the code. In an attempt to pull this logic into an easier to understand form and to provide a snapshot of the algorithm requirements, Algorithm Enunciation Language (AEL) was used. Through a series of meetings between researchers, software developers working with the researchers, AEL authors, and software developers tasked to produce maintainable operational code, a process commonly referred to as a code walkthrough was used with a slight modification. AEL authors would take the research code, remove debug statements, indent and color code different levels of decision logic, and finally insert drafts of the AEL directly above the corresponding research code. During the code walkthrough which was moderated by the AEL authors, researchers and research software developers could compare and confirm the research code against the AEL, while operational software developers followed the logic from one block of AEL to the next. After these meetings the final AEL documentation was created and software developers began writing the operational code. Finally, NSSL data sets were used to validate results between the research code and the operational code. As the first dual polarization WSR-88D's are deployed, this validation will continue on operational data sets.

3.3 *Preprocessing Algorithms*

On each elevation cut, the RDA will provide radials containing base data fields (conventional moments and dual polarization variables) at the same azimuth resolution. Beginning in build 10, this azimuth resolution became 0.5 degree on the low elevation split cuts scans. The dual polarization radar research and algorithm development at NSSL was based on collecting and processing data of 1 degree azimuthal resolution. It is believed that such spatial resolution is appropriate for the IOC dual polarization algorithms and products. To maintain the same data quality and algorithm performance as that demonstrated in the research and development, 0.5 degree data is recombined to create 1 degree data before algorithm processing.

The RPG uses an algorithm developed at NSSL for recombining dual polarization data (ROC 2820003, 2009). For each 1 degree azimuthal resolution range gate, the algorithm performs a linear combination of the complex covariance values calculated for the pair of 0.5 degree azimuthal resolution gates at that range. This resultant combined complex covariance array is then used to calculate the recombined moments for correlation coefficient, differential phase and differential reflectivity.

The differential phase field as generated in the RDA is in the range of 0 to 360 degrees, and any value that is outside the range is aliased, or "wrapped". We must unwrap the data before it can be used, for example, for calculating the specific differential phase (Kdp). The unwrapping algorithm in the RPG was developed at NSSL (ROC NX-DR-03-061, 2009). It is based on the assumption that the differential phase must change gradually along the radial.

The recombined and unwrapped dual polarization data are then preprocessed before being passed to the algorithms. Dual polarization fields and base moments are smoothed along the radial to reduce the variances introduced by the noise and ground clutter contamination. The reflectivity and the differential reflectivity are corrected with the differential phase. The specific differential phase is estimated. The signal-to-noise ratio and the spatial variability (the texture) of both the reflectivity and the differential phase are calculated. These are required inputs for the dual polarization algorithms -- data quality index, melting layer detection, hydrometeor classification, and quantitative precipitation estimation.

3.4 *Base Data Products*

The RPG will produce three new base data products from the recombined and preprocessed dual polarization base data fields. Each product will be available in both 16 data levels and 256 data levels, which will be provided at 1 km and 0.25 km range resolution, respectively. Default color tables were designed so that important data value transitions are apparent, that the product type is quickly recognized and not mistaken for existing product types. The reflectivity field corresponding to the following dual polarization base product examples is shown in Figure 1.

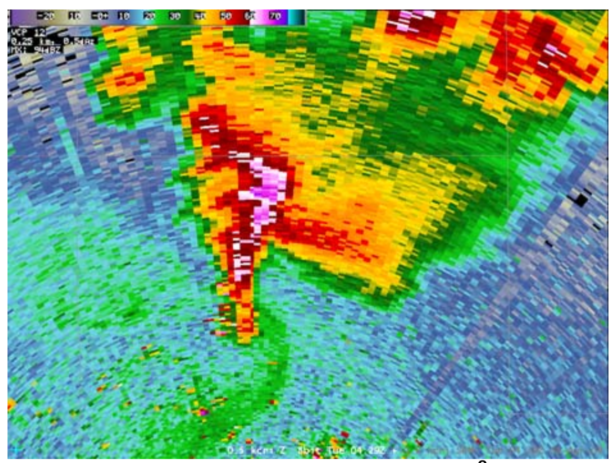

Figure 1 KOUN, 4/8/2008, Z product at 0.5^{o} elevation.

3.4.1 *Differential Reflectivity (Zdr)*

Differential reflectivity is the ratio of the reflected horizontal and vertical power returns and expressed in decibels. It is a good indicator of the median shape of the reflecting particles, which in turn can be a good estimate of particle size. Differential reflectivity can be useful in detecting hail, the location of updrafts, the melting layer and some non-meteorological scatterers (Scharfenberg and Manross, 2007).

To generate the differential reflectivity product, the RPG uses data from its dual polarization preprocessor, not directly from the RDA. The RPG's dual polarization preprocessor modifies the raw differential reflectivity data from the RDA by smoothing it, then applying a correction for horizontal attenuation and system calibration. Figure 2 contains a Zdr product for the same time and elevation as the reflectivity product in Figure 1.

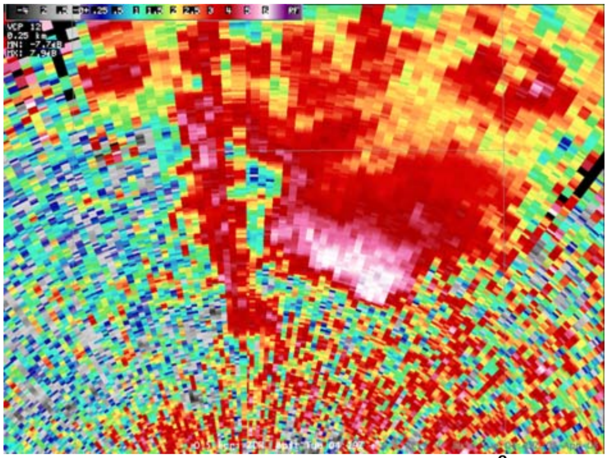

Figure 2 KOUN, 4/8/2008, Zdr product at 0.5°.

3.4.2 *Correlation Coefficient (CC)*

Correlation coefficient is a dimensionless measure of the similarity between the reflected horizontal and vertical power returns within each radar sample bin. This is an indicator of the homogeneity of scatterers within the sample volume, where values close to 1.0 are nearly uniform. Areas with low correlation coefficients are a good indicator of regions of mixed precipitation types, non-meteorological scatterers, or large hail. Correlation coefficient products have non-linear data levels to enhance discrimination of correlation coefficient values near 1.0, the upper end of the data range. In this region it is important operationally to distinguish small variations of correlation coefficient to help in identifying the extent of the melting layer, regions of mixed phase precipitation and the presence of non-meteorological echoes. Low correlation coefficients in meteorological echo can be indicative of very large hail. Figure 3 contains the CC product corresponding to Figure 1.

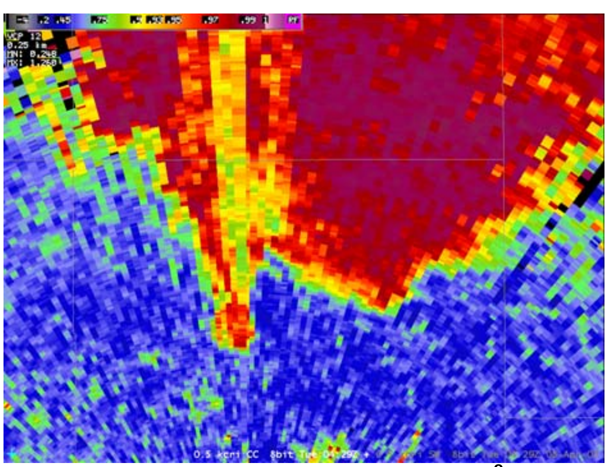

Figure 3 KOUN, 4/8/2008, CC product at 0.5°.

3.4.3 *Specific Differential Phase (Kdp)*

Specific differential phase is derived by the RPG's dual polarization preprocessor using the differential phase obtained from the RDA. The specific differential phase is the derivative of the differential phase over approximately 2 to 6 kilometers (based on signal strength) along each radial. That is, it is a measure of the rate of change in differential phase as the radar signal propagates through the atmosphere and intercepts various hydrometeors along the way. Specific differential phase is strongly related to rain rate and has the desirable quality of being insensitive to radar calibration, partial beam blockage, propagation effects, system noise, and the presence of hail (Brandes, 2000). This makes specific differential phase useful for precipitation estimation when partial beam blockage is present and rain rates are high. Figure 4 contains the Kdp product corresponding to Figure 1.

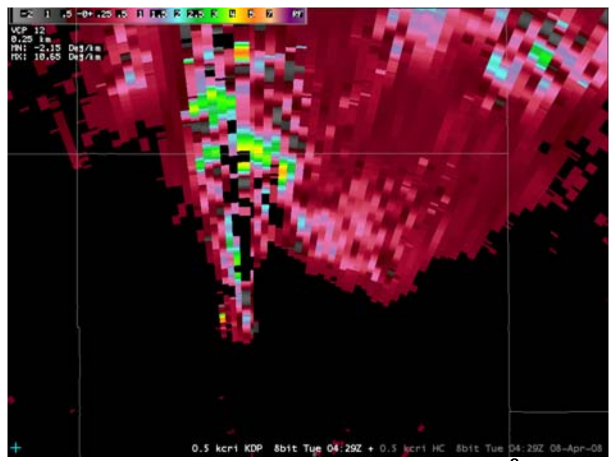

Figure 4 KOUN, 4/8/2008, Kdp product at 0.5°.

3.5 *Hydrometeor Classification Algorithms*

3.5.1 *Quality Index Algorithm (QIA)*

A normalized estimate of data quality is needed by the HCA for six of the HCA's input dual polarization data fields.

The quality index is an estimate of the radar signal's vulnerability to the following five factors: attenuation, non-uniform beam filling effects, magnitude of the correlation coefficient, signal-to-noise ratio and partial beam blockage. A data field with a quality index value of anything less than 1.0 indicates the data is degraded by one or more of the five factors.

The QIA computes a quality index value at every radar sample bin for the following six data fields: reflectivity, differential reflectivity, correlation coefficient, specific differential phase, texture of reflectivity and texture of differential phase. Interestingly, the quality index for each of these six data fields can be computed using only the differential phase, correlation coefficient and signal-to-noise ratio (SNR), all obtained from the dual polarization preprocessor algorithm.

In general, to compute quality indexes the differential phase, correlation coefficient and SNR for a given radar sample bin are divided by a constant value that has been empirically determined for each of the three input fields. The quotients are then squared, the results are added together and the sum, s, is inserted into the following formula:

$$\text{Quality Index} = e^{(-0.69s)}$$

The following section describes how the HCA uses the quality index, in combination with fuzzy logic, to determine a hydrometeor type for every radar sample bin.

3.5.2 *Hydrometeor Classification Algorithm (HCA)*

The HCA employs a fuzzy logic scheme using six input radar data fields (both single and dual polarization base data) to classify each radar sample bin as one of the following 12 categories:

GC Ground clutter/anomalous propagation
BI Biological
DS Dry snow
WS Wet snow
IC Ice crystals
BD Big drops
RA Rain (light and moderate)
HR Heavy rain
GR Graupel
HA Hail (mixed with rain)
UK Unknown
ND No data (less than threshold)

The HCA also uses output from the MLDA to refine further the classification possibilities for a given radar sample bin.

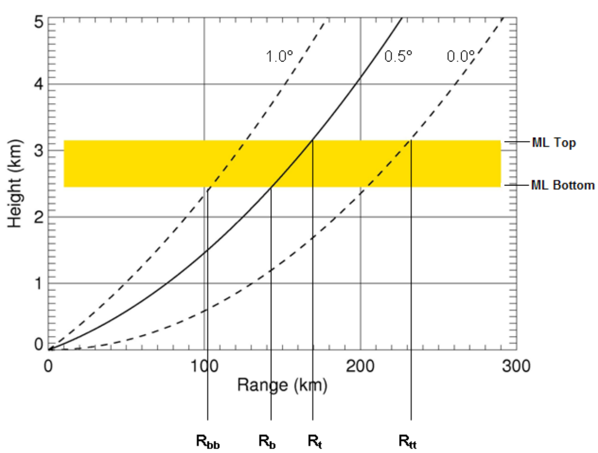

Figure 5 Geometry of Radar Beam and Melting Layer

For each radar elevation angle, the melting layer (i.e., area between ML Top and ML Bottom) is geometrically projected onto the radar beam (see Figure 5) to determine the following locations:

1) Where the top of the beam intersects the bottom of the melting layer (R_{bb})
2) Where the center of the beam intersects the bottom of the melting layer (R_b)
3) Where the center of the beam intersects the top of the melting layer (R_t)
4) Where the bottom of the beam intersects the top of the melting layer (R_{tt})

These four locations define five regions along a radial of radar data that describe the beam as being either completely below, partly below, mostly within, partly above, or completely above the melting layer. Using the two-letter abbreviations from the list above, the allowable hydrometeor classes within each region relative to the melting layer are:

Completely below:
GC, BI, BD, RA, HR, HA, UK, ND
Partly below:
GC, BI, WS, BD, RA, GR, HR, HA, UK, ND
Mostly within:
GC, BI, DS, WS, BD, GR, HA, UK, ND
Partly above:
GC, BI, DS, WS, IC, BD, GR, HA, UK, ND
Completely above:
DS, IC, GR, HA, UK, ND

For each radar sample bin, the HCA combines fuzzy logic processing and a matrix of weighting factors for each input variable and each hydrometeor class to compute an aggregate score for each allowable hydrometeor classification. The highest aggregate score determines the class designation for that radar sample bin. If no aggregate score meets the minimum threshold, a classification of UK (Unknown) is assigned to the radar sample bin. The weighting factors enable some input variables to have greater (or less) influence on the classification than others. For example, since ground clutter (GC) is best identified by the correlation coefficient field, its GC weighting factor for correlation coefficient is 1.0 (the maximum possible). Whereas, the GC weighting factor for differential reflectivity is 0.4 because it is less effective at identifying clutter. By setting a weighting factor to zero, the impact of a fuzzy logic input variable is eliminated. This is done in the case of specific differential phase and the classifications for dry and wet snow. Studies have shown that specific differential phase is not a good discriminator for snow (Ryzhkov and Zrnic, 1998).

In addition, several "hard rules" are applied to prevent obvious misclassifications. For example, a hail classification is not permitted in a radar sample bin with reflectivity below 30 dBZ and a biological classification is not permitted in a radar sample bin with a correlation coefficient greater than 0.97.

3.5.3 *Melting Layer Detection Algorithm (MLDA)*

The MLDA identifies the top and bottom boundaries of the melting layer for use by the HCA. The MLDA estimates the top and bottom height of the melting layer by identifying regions of wet snow, which is the dominant hydrometeor type in the melting layer.

Although the MLDA receives HCA output, it does not directly use the HCA's wet snow classification. Rather, the MLDA uses HCA output only to eliminate radar sample bins classified as ground clutter, biological, unknown and no data from its search for wet snow. In the remaining radar sample bins, reflectivity and correlation coefficient are examined for lower and upper limit thresholds typically found in a melting layer. These thresholds are currently defined as 15 dBZ to 47 dBZ for reflectivity and 0.90 to 0.97 for correlation coefficient. Finally, radar sample bins that are less than 6 kilometers above radar altitude and having a signal-to-noise ratio above 5 dB are searched for signatures that coincide with the melting layer which are maxima in reflectivity and differential reflectivity and a minimum correlation coefficient (Brandes and Ikeda, 2004). If these wet snow criteria are met, a wet snow data point at that azimuth angle is saved and given a weight, based on the elevation angle, to create a wet snow score. Wet snow data points at higher elevation angles are considered more reliable than those at lower altitudes. The MLDA only processes elevation angles from 4.5 to 10 degrees. These angles have the most pronounced melting layer signatures and they minimize the impact of ground clutter contamination (Giangrande, et al., 2005).

Weighted wet snow scores at each azimuth angle are added to a histogram of scores saved from the current and past two volumes scans (if available). This histogram is then used to determine the melting layer top, defined as the height below which is 80% of the total wet snow score. The melting layer bottom is defined as the height below which is 20% of the total wet snow score. Finally, a smoothing process is performed using a running 21 degree azimuth window (the current azimuth and 10 degrees either side) to minimize azimuthal discontinuities.

If the total wet snow score is insufficient to estimate the melting layer, the MLDA simply uses the height of the 0° C isotherm as the melting layer top and subtracts 500 meters to obtain the melting layer bottom height. The 0° C isotherm height is obtained from the Rapid Update Cycle (RUC) model data which is input hourly to the RPG from an associated AWIPS. If the RUC model is not available, the 0° C height adaptable parameter, which is manually entered at the RPG and also used by the Hail Detection Algorithm (HDA), is used.

3.6 *Hydrometeor Classification Products*

3.6.1 Hydrometeor Classification Product *(HC)*

This derived product contains the result of HCA processing at each elevation angle of the volume scan. For consistency with other products the RPG produces both 16 and 256 data level versions, although both contain only 12 valid classes as described in the Hydrometeor Classification Algorithm section above. The 256 data level product is at 0.25 km range resolution, while the 16 data level product is at 1 km range resolution which is derived by first smoothing the data with a range oriented 9 sample bin mode filter (Mode-9) and then using every 4th sample bin to format the product. Figure 6 shows the HC product corresponding to the same time and elevation as Figure 1.

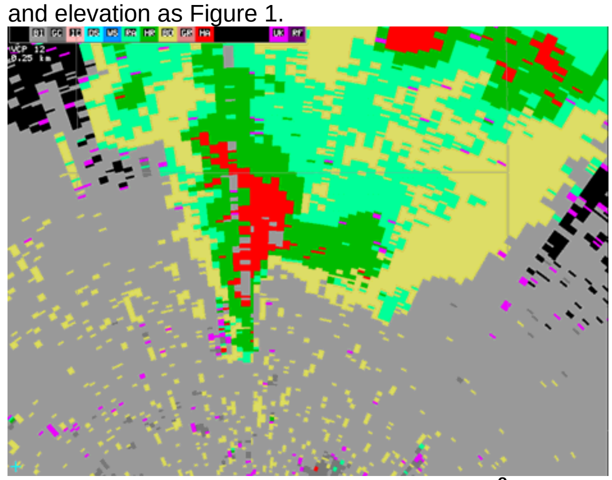

Figure 6 KOUN, 4/8/2008, HC product at 0.5^o.

3.6.2 Melting Layer Product *(ML)*

This elevation-based overlay product graphically shows the locations where the radar beam intersects with the melting layer as determined by the MLDA. In a typical meteorological situation with an elevated melting layer, the product consists of four lines, each describing an approximate circle. Closest to the radar is a dashed circle representing the point along the radial where the top of the radar beam first intersects the bottom of the melting layer. In the region from the radar to this first dashed line, the radar beam is entirely below the melting layer and contamination from frozen hydrometeors is not expected. Next, two solid line circles represent the beam center's intersection with the bottom and top of the melting layer, respectively. An outer dashed circle represents the point along the radial beyond which the beam is entirely above the melting layer. The ML product is shown in Figure 7 displayed as an overlay on a correlation coefficient product.

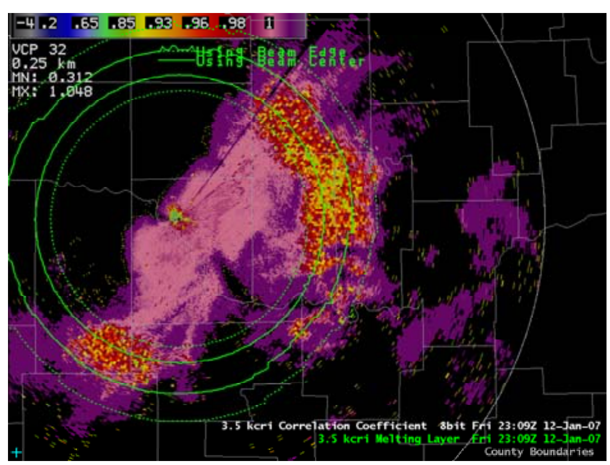

Figure 7 KOUN, 1/12/2007, Melting Layer product overlay on a CC product at 3.5^o elevation angle.

3.7 *Quantitative Precipitation Estimation (QPE) Algorithm*

Like its legacy single polarization predecessor, the Precipitation Preprocessing Subsystem (PPS), the polarimetric QPE algorithm receives data one elevation at a time and uses it to construct a hybrid scan of radar-based data. The QPE algorithm builds the hybrid scan based on terrain data and the hydrometeor classes from the HCA. This hybrid scan is composed of precipitation rate data (vs. reflectivity for the PPS).

As opposed to the PPS, where only reflectivity is used to compute precipitation, QPE uses dual polarization moments, HCA hydrometeor classes, and MLDA information to compute rates. To smooth out non-meteorological variability, the QPE algorithm determines the most frequent value (statistical mode) of nine adjacent radar sample bins along each radial, called a Mode-9 filter, and applies this filter to each elevation of HCA data while constructing the hybrid scan.

QPE considers each 250 m radar sample bin individually and determines whether it can be used to compute a precipitation rate. This decision is based primarily on the hydrometeor class assigned by the HCA. At each radar sample bin within the polar grid surrounding the radar, for hydrometeor classes Ground Clutter (GC) or Unknown (UK), the radar sample bin is not used and an attempt is made to compute a valid precipitation rate from data at a higher elevation. When hydrometeor classes Biological (BI) or No Data (ND) are encountered, a valid precipitation rate of 0.0 is assigned to that radar sample bin. Finally, if CC is low (< 0.85 by default) or if the radar beam is blocked more than a predetermined usability threshold (70% by default), the radar sample bin is not used, and an attempt is made to compute a valid precipitation rate from data at a higher elevation.

QPE uses the hydrometeor classes and the radar sample bin's height relative to the melting layer to determine how to compute the precipitation rates. Below is a list of precipitation rate formulas used for each hydrometeor class:

0 [mm hr^{-1}]	nonmeteorological echo (BI, ND)
$R(Z, Z_{DR})$	Light/Moderate Rain (RA)
$R(Z, Z_{DR})$	Heavy Rain or Big Drops (HR, BD)
$R(K_{DP})$	Hail, mixed with rain (HA) below the top of the melting layer
0.6 * R(Z)	Wet Snow (WS)
0.8 * R(Z)	Graupel (GR)
0.8 * R(Z)	Hail, mixed with rain above the top of the melting layer
R(Z)	Dry Snow (DS) below the top of the melting layer
2.8 * R(Z)	Dry Snow (DS) above the top of the melting layer
2.8 * R(Z)	Ice Crystals (IC)

Similar to the PPS, as each radar sample bin is filled with rate data, QPE computes the surface area exceeding a threshold precipitation rate. At the beginning of a precipitation event, when the area first exceeds a threshold area, QPE initiates the storm total accumulation. At the end of a precipitation event, after an hour of no precipitation, the storm total accumulation is ended.

The QPE algorithm should improve precipitation estimation in the following situations:

- where the radar beam is partially blocked
- for nearly all hydrometeor classes (all except dry snow below the top of the melting layer)
- by greatly reducing non-precipitating echoes (such as ground clutter and biological scatterers) that contaminate PPS estimates
- by identifying the bright-band (melting layer)
- by showing rain/snow discrimination and
- by identifying hail and mitigating hail contamination

3.8 *Precipitation Products*

All dual polarization precipitation products are new. However, the existing PPS products will remain in WSR-88D for at least a few years after dual polarization is fully deployed. All the new dual polarization products: a) are polar grids, b) have a maximum range of 230 km and c) have an azimuthal resolution of 1 degree. Below is a brief description of each of the new dual polarization precipitation products generated by the QPE algorithm.

3.8.1 *One-Hour Accumulation (OHA) and Digital Accumulation Array (DAA)*

The OHA and DAA products are an estimate of precipitation accumulation over the last hour in inches. Figure 8 contains an example of an OHA product.

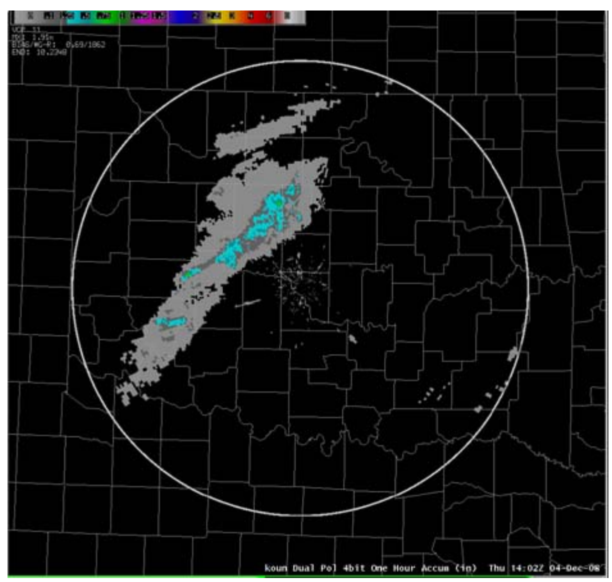

Figure 8 KOUN, 6/10/2003. OHA product on AWIPS.

The OHA product has 16 data levels (i.e. 4-bit) which are adaptable and a range resolution of 2 km. The DAA product has 256 data levels (i.e. 8-bit) and a range resolution of 0.25 km. The DAA will never have a rain-gage bias correction applied (within the RPG), but the OHA and other QPE accumulation products can potentially have bias applied.

3.8.2 *Storm Total Accumulation (STA) and Digital Storm Total Accumulation (DSA)*

The STA and DSA products are both an estimate of the precipitation accumulation since the beginning of a precipitation event (as determined by the QPE). The STA product has 16 data levels (i.e. 4-bit) which are adaptable and a range resolution of 2 km. The DSA product has 256 data levels (i.e. 8-bit) and a range resolution of 0.25 km. If there has not been any precipitation in the last hour, the products are empty (i.e., they show no accumulation). The products also includes adaptable parameter values, rain-gage bias information (for future implementation), and other supplemental (precipitation status) data. Figure 9 contains an example of an DSA product.

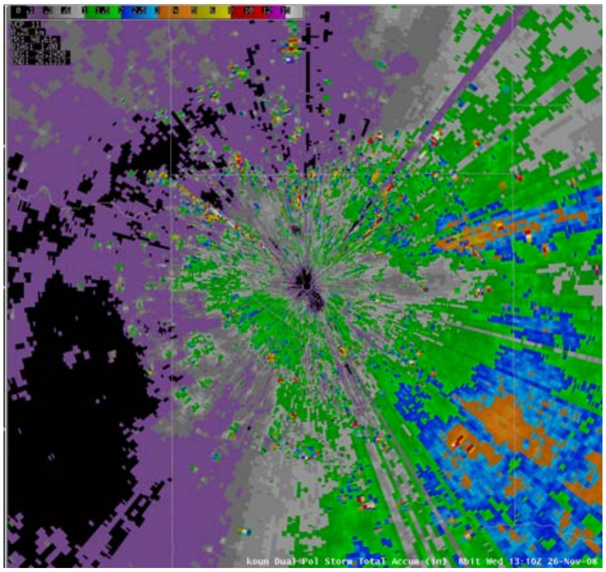

Figure 9 KOUN, 6/10/2003, DSA product zoomed-in near the radar.

3.8.3 *Digital User-Selectable Accumulation (DUA)*

The DUA product is an estimate of precipitation accumulation over a user-selected accumulation period. The accumulation period is of variable duration and defined via two parameters: the ending time (Z) in hh:mm format, and the time span in hh:mm format (ranging from 15 minutes to 24 hours prior to the ending time). The product will usually be generated by request, but will also be generated daily by default at 12Z for a time span of 24 hours and every volume scan for a time span of 1 hour. The DUA product has 256 data levels (i.e. 8-bit) and has a range resolution of 0.25 km.

3.8.4 *Digital Instantaneous Precipitation Rate (DPR)*

The DPR is a polar grid of digital high-resolution instantaneous precipitation rates. The product has 65,536 data levels (i.e. 16-bits) and has a range resolution of 0.25 km. Figure 10 shows an example of a DPR product at the same date and time as shown in Figure 8.

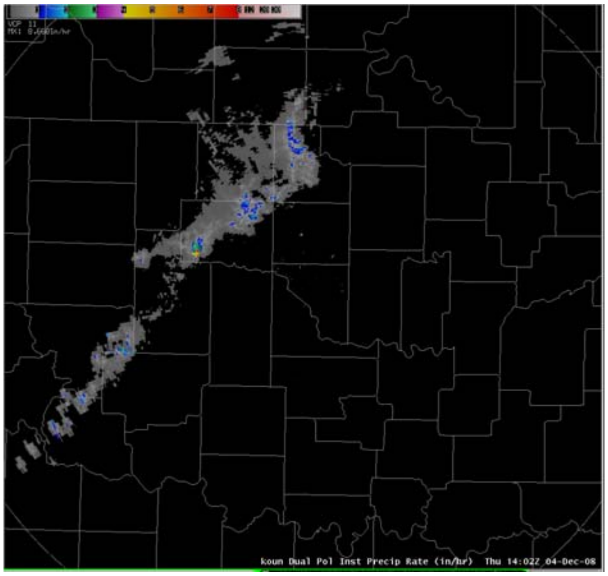

Figure 10 KOUN, 6/10/2003, DPR product.

3.8.5 *Hybrid-Scan Hydrometeor Classification (HHC)*

The HHC product contains the hydrometeor classification for each radar sample bin used in the QPE hybrid scan each volume scan. Since the QPE applies the Mode-9 filter to HCA data, this product will often resemble the 16 data level HC product at the elevation angle used in the hybrid scan. The product has 16 data levels and a range resolution of 0.25 km. (See Figure 11).

Figure 11 KOUN, 6/10/2003, HHC product.

3.8.6 *Digital One-Hour Difference (DOD) and Digital Storm Total Difference (DSD)*

The DOD and DSD are polar grids of digital accumulation differences computed by subtracting the estimates computed by the PPS from estimates computed by the QPE. The DOD is a difference of one-hour-estimates, and the DSD is a difference of storm total estimates. Both products have 256 data levels (i.e. 8-bits) and have a range resolution of 0.25 km. The DSD product will be blank if the PPS and QPE storm totals are blank. An example DSD product is shown in Figure 12, which depicts the difference between Figure 9 and Figure 13. The shades of purple show where clutter contamination was reduced by the QPE.

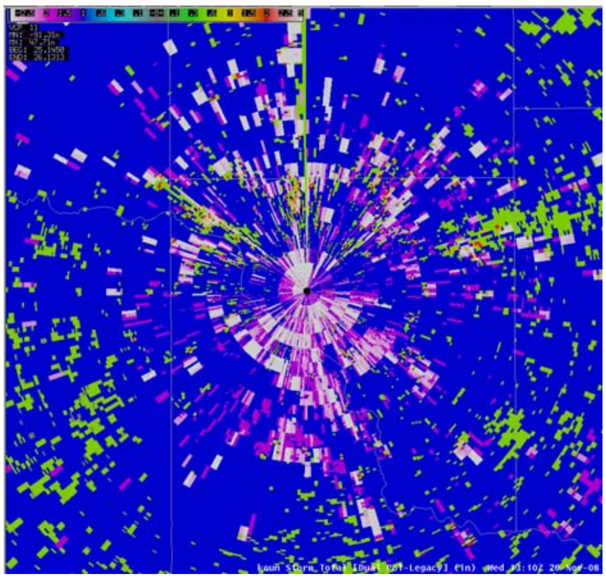

Figure 12 KOUN, 6/10/2003, DSD product zoomed-in near the radar.

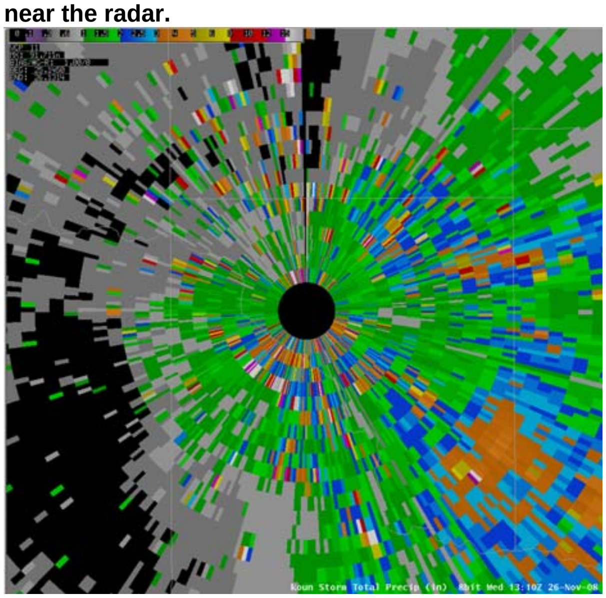

Figure 13 KOUN, 6/10/2003, DSP product from legacy PPS zoomed-in near the radar.

4. AWIPS CAPABILITIES FOR DUAL POLARIZATION WSR-88D

The AWIPS OB9 includes software enhancements to display dual polarization radar data. Many of the capabilities described below are generic display applications and therefore will be available to forecasters long before the radars are upgraded.

4.1 *Reorganized Radar Menus*

The first major change to the AWIPS software is a reorganization of the radar menus. There have been several product additions and removals over the past 8 years and dual polarization will change the concept of operations significantly, therefore radar menus got a top down redesign. When the RDA is upgraded to dual polarization capability, an AWIPS turnkey script will be run that modifies the radar menus to what is shown in Figure 14. The new radar menus are better organized and more elegant than those prior to dual polarization, and also support new ways to display the products.

Figure 14 Reorganized AWIPS Radar Product Menu

4.2 *Four-Panel Display Operations*

New product displays include the ability to load a 4-panel layout of radar products and manipulate them using the familiar "All-Tilts" functionality, whereby the user can go forward and backward in time, and up and down in radar elevation angle, keeping the 4 displayed products synchronized. Though 4-panel "All-Tilts" displays are a nice way to analyze dual polarization data, the small size of the each of the 4 windows is a limitation even after zooming into the products. To overcome this limitation, a new display capability labeled "Panel/Combo Rotate" is available (see Figure 15).

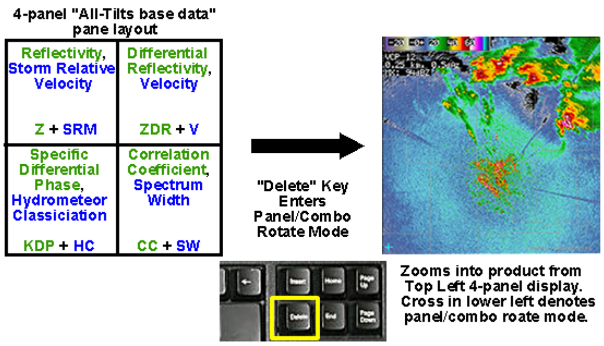

Figure 15 Illustration of Panel/Combo Rotate given that the "All-Tilts base data" multi-load is loaded first (left side of figure).

From the 4-panel "All-Tilts" display, hitting the "Delete" key on the keyboard will zoom to a single pane view of the radar product that is located in the top left of the 4-panels. With "Panel/Combo Rotate" the single pane display retains the All-Tilts capability, and you can also quickly toggle between the other products that were originally loaded in the 4-panels using the number keys on the keyboard (See Figure 16).

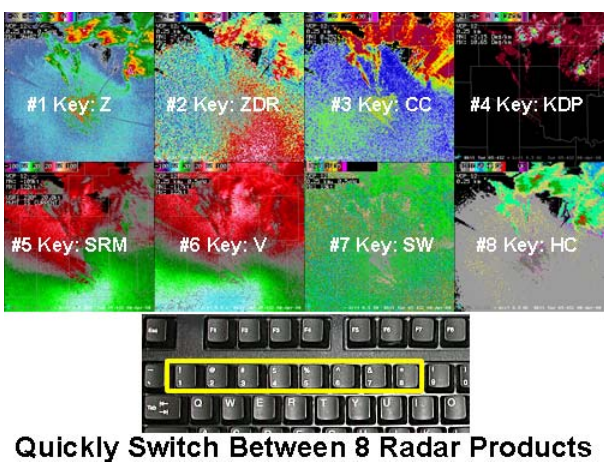

Figure 16 With the multi-load in Figure 15, while in Panel/Combo Rotate mode, the keys inside the yellow rectangle correspond to the products shown in this graphic.

In "Panel/Combo Rotate", the #2 key displays the top right, the #3 key displays the bottom right, and the #4 key displays the bottom left radar products respectively (see Figure 16). The ability to quickly toggle products is not limited to 4 products, however. If the user loads image combinations into each of the original 4-panels, then keys 5-8 are used to toggle to them. Thus, the ability to quickly toggle between all the dual polarization base products is possible.

Additional functionality paired with "Panel/Combo Rotate" is the "All Panel Sample". While in panel combo rotate, enabling "All Panel Sample" will allow the user to view data values of the hidden products in the cursor readout (Figure 17).

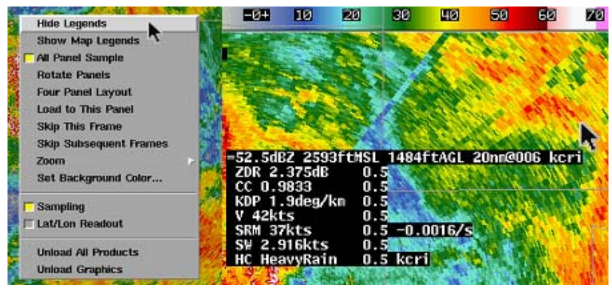

Figure 17 Holding down right click, which in panel/combo rotate mode, allows for All Panel Sample to be turned on (left), which, reveals the corresponding values of all panels (right).

For example, with the main AWIPS pane displaying reflectivity and "All Panel Sample" turned on, cursor readout would display not only the reflectivity values at the tip of the mouse pointer, but also the corresponding values of differential reflectivity, correlation coefficient, specific differential phase, hydrometeor classification output, mean radial velocity, etc. Every product loaded as part of the 4-panel display (as many as 8 radar products) will be visible in the cursor readout in "Panel/Combo Rotate" mode with "All Panel Sample" turned on.

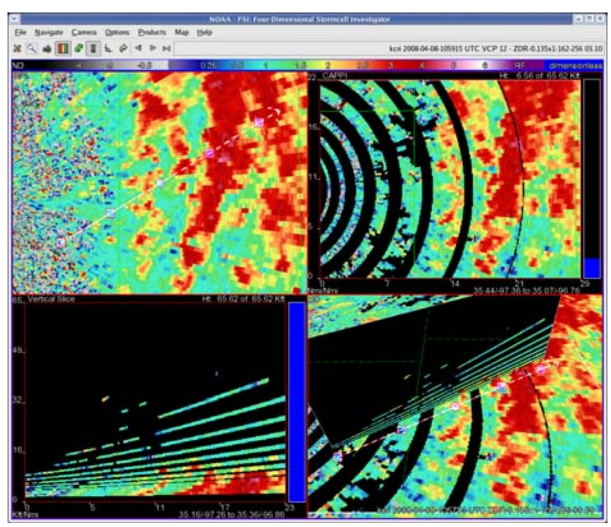

Figure 18 FSI showing ZDR.

4.3 *Additional Enhancements*

There are additional enhancements to OB9 in support of the dual polarization upgrade. The Four Dimensional Storm Investigator (FSI) is modified to display dual polarization products (Figure 18). This is especially useful for cross sectional analysis, a tool vital to integrating dual polarization radar products into the forecast process. Dual polarization product mosaics are available for each of the base moments, the hydrometeor classification, and several of the rainfall estimation products.

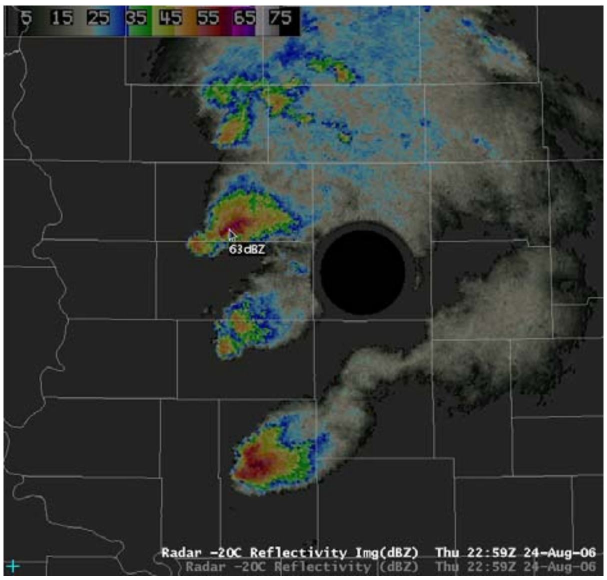

Figure 19 Reflectivity CAPPI at the -20 deg. C level.

Finally, the AWIPS volume browser is modified to include the ability to display Constant Altitude Plan Position Indicators (CAPPIs) of several radar products either at a height above radar level, above mean sea level, or at a temperature level (e.g., -20°C in Figure 19).

5. CENTRAL COLLECTION AND DISTRIBUTION OF DUAL POLARIZATION INFORMATION

WSR-88D Level II data consists of volume scans of base data radials and metadata, whereas Level III refers to products generated by the RPG from Level II and other data. Dual polarization will add a considerable quantity of data to the communication networks, servers, and storage systems responsible for the central collection, distribution, and archive of WSR-88D Level II data and Level III products.

5.1 *Level III Products*

WSR-88D Level III products are centrally collected, distributed via Radar Product Central Collection and Dissemination Service (RPCCDS) and the NOAAPORT satellite broadcast system (SBN), and archived at NCDC. Data throughput varies widely with weather and Volume Coverage Pattern (VCP). It currently ranges from 3 to 21 kbps per radar, resulting in a total network hourly average peak load near 1.6 mbps. Depending on the type of products added, the number of elevations, and the resolution, with dual polarization this load is estimated to at least double. Figure 20 lists the product mnemonic, message code, resolution, range and other descriptive information for the full IOC dual polarization product suite.

Technical Requirements for the WSR-88D Dual Polarization Products rev14 3jun2008-mji			Dual Polarization Base Products						HCA			Quantitative Precip Est(QPE)								
			Differential Reflectivity (db)		Correlation Coefficient		Specific Differential Phase (deg/km)		Hydrometeor Classification		Melting Layer	Hybrid-Scan Hydrometeor Classification	Digital Inst. Precip Rate (in/hr)	One Hour Accum	Dig. Accum Array (G-R bias never applied)	Storm Total Accum		Digital User-Selectable Accum	Dig. One-Hour Difference Accum	Dig. Storm Total Difference Accum
Product Characteristics	Product Mnemonic and Message Code (#)	RPG	DZD	ZDR	DCC	CC	DKD	KDP	DHC	HC	ML	HHC	DPR	OHA	DAA	STA	DSA	DUA	DOD	DSD
		#	159	158	161	160	163	162	165	164	166	177	176	169	170	171	172	173	174	175
		AWIPS	ZDR		CC		KDP		HC		ML	HHC	DPR	OHA	DAA	STA		DUA	DOD	DSD
	RPG ICD Packet Code		16	af1f	16	af1f	16	af1f	16	af1f	e03,802	16	28	af1f	16	af1f	16	16	16	16
	Number of Data Levels		256	16	256	16	256	16	256	16	4	16	65536	16	256	16	256	256	256	256
	Azimuth Resolution	deg	1	1	1	1	1	1	1	1	1	1	1	1	1	1	1	1	1	1
	Range Resolution	m	250	1000	250	1000	250	1000	250	1000	250	250	250	2000	250	2000	250	250	250	250
	Compression Method		BZ2	rle	BZ2	rle	BZ2	rle	BZ2	rle		BZ2	BZ2	rle	BZ2	rle	BZ2	BZ2	BZ2	BZ2
	Maximum Range	km	300	230	300	230	300	230	300	230	230	230	230	230	230	230	230	230	230	230
	Generation Frequency	E/V	Elev		Elev		Elev		Elev		Elev	Vol	Vol	Vol	Vol	Vol	Vol	Vol, otr	Vol	Vol
	Minimum, Maximum Data Values & (precision)		-7.9,7.9 (.0625)	-4,6 (.25-3)	0.2,1.05 (.00333)	0.2,1.05 (.01-.25)	-2,I0 (.05)	-2,7 (.25-3)	n/a	n/a		n/a	0.0,65.535 (0.001)	like PPS OHP	1*	like PPS STP	1*	1*	2*	2*
Sizing	Uncompressed Product Storage Size (Kilo bytes)	min	93	same as xmit	93	same as xmit	93	same as xmit	93	same as xmit	0.1	0.1	0.1	0.1	0.1	0.1	0.1	0.1	0.1	0.1
		max	337		337		337		337		6	331	663	21	331	28	339	331	331	331
		avg	236		236		236		236			331	663	21	331	28	339	331	331	331
	Product Transmission Size (Kilo bytes) during Widespread Svr Wx	min	33	27	28	25	11	17	8	12	5	8.9	140	11		10.9	62.7	55.6	51.9	52.9
		max	103	29	86	27	51	20	23	13	5	11	151.4	12.0	165.5	10.9	62.8	64.7	58.2	53.0
		avg	80	28	66	26	33	18	17	12	5	9.8	144.7	11.4	132	10.9	62.8	61.8	54.8	53

(1) an adjusting range of data and precision, based on the maximum data value. (2) adjusting range of data and precision, based on the maximum absolute value of the data and with equal precision and data range for both positive and negative values.

Figure 20 WSR-88D Dual Polarization Product Characteristics

The dual polarization products selected for collection will likely include a few elevations of the base data and hydrometeor classification products and QPE products which parallel the current suite of rainfall accumulation products. Analysis is underway to define specific product collection requirements to support a dual polarization radar concept of operations.

5.2 *Level II Data*

Level II data is centrally collected in near real-time from 135 radars, distributed to external users by top tier sites, and archived at the National Climatic Data Center (NCDC). The super-resolution enhancement deployed with Build 10 drove several changes to the Level II data. On the low elevation split cuts, super-resolution increased the azimuthal resolution to 0.5 degrees and increased the range resolution of reflectivity data to 0.25 km, and extended the range of Doppler data to 300 km. The format for base data radials is called Message 31. The migration to Message 31 was needed to support the larger size of base data radials and version numbers are used to distinguish super-resolution from recombined resolution base data. The Message 31 format was designed to also support adding data fields like dual polarization and is described in RDA to RPG Interface Control Document (ROC 2620002, 2009).

The data throughput of Level II varies widely with weather and Volume Coverage Pattern (VCP). With Build 10 super-resolution, it currently ranges from 10 to 180 kbps per radar, resulting in a total network hourly average peak load near 7 mbps. With dual polarization IOC this load is estimated to double.

Currently, where communications bandwidth is not adequate to support distribution of super-resolution Level II data, recombined data is distributed. This is now done at DOD and DOT WSR-88Ds Level II sites because of resource constraints and we are exploring options on how to provide the additional data. The bandwidth allocated for Level II data is 384 kbps to carry super-resolution data and 128 kbps for recombined data. During fast VCPs and widespread weather, the throughput of full resolution dual polarization Level II data could exceed 384 kbps. Therefore to prevent a significant impact to latency, a bandwidth upgrade that would provide an allocation of 512 kbps is needed at all sites. If resource constraints continue in the dual polarization era, distribution of recombined dual polarization Level II data will be necessary. Furthermore, if communications links where distribution of recombined super-resolution data is currently being performed (i.e., DOD and DOT WSR-88D's) are not upgraded, then dual polarization base data will be removed from the Level II data. New version numbers will be introduced to distinguish full resolution dual polarization data from the other types of reduced resolution data.

6. FUTURE PLANS

6.1 *Algorithm Development*

HCA was originally developed for warm-season weather. Additional work is needed to optimize its performance for transitional and winter weather. There is evidence that MLDA requires adjustment for cold-season storms if the height of the freezing level is below 1 km above ground (Boodoo et al. 2008). One possible way to address the problem is to utilize vertical profiles of thermodynamic variables retrieved from numerical forecast models in combination with polarimetric radar data.

Another challenge for HCA is the need to increase the number of classes by splitting the existing broad category "rain / hail mixture" into small hail and large hail and adding the category of freezing rain which is of great concern during winter storms. More emphasis on winter weather will require more comprehensive analysis of polarimetric data collected during cold season. In this regard, it would be beneficial for this analysis to utilize polarimetric data collected by existing C-band radars in the northern part of the US and Canada.

Accurate measurements of precipitation at longer distances from the radar and in the presence of beam blockage still remain a problem. In both situations, the radar overshoots precipitation; hence efficient procedures for the retrieval of vertical profiles of precipitation have to be developed. A polarimetric vertical profile of rain based on microphysical modeling of precipitation formation and evolution is in order. Quantitative estimation of snow with polarimetric radar is another frontier of research.

Furthermore, the identification of the location of convective cells in the radar volume can be utilized by the HCA in projecting localized areas with higher melting levels and different hydrometeor characteristics.

6.2 Software Implementation

For the QPE algorithm, there are plans to upgrade the technique which accounts for retrieving precipitation estimates in partially blocked area. In addition, there are plans to have a rain gage bias correction applied to QPE products and for the AWIPS Multi-sensor Precipitation Estimator (MPE) which computes the gage bias to ingest dual polarization products.

6.3 Infrastructure

After dual polarization deployment is underway, the RDA Build 12 software will be merged with Build 11 which includes the Clutter Mitigation Decision (CMD) function. CMD is an automation technique designed to mitigate transient clutter returns on the split cut scans at low elevation angles. This automatic detection and filter application process reduces dependence on static clutter bypass maps and eases the need for operators to manually apply filtering under anomalous propagation conditions. Currently, CMD can only use the horizontal polarization time series data, but development is underway to customize CMD for dual polarization and use both the horizontal and vertical time series data plus extend CMD to all elevation angles.

6.4 Applications

New applications are being developed which take advantage of polarimetric data which automatically identify and assess features and improve data quality. Some examples would be tornado debris cloud, bird-specific data, and hail size. Other algorithms will use the polarimetric data to improve derived products such as snowfall, liquid water equivalent and in-flight icing estimations. Related applications would include provision of velocity and spectrum width data with bird returns removed, and inclusion of polarimetric hydrometeor classification information in AP and ground clutter mitigation schemes.

7. SUMMARY

Full thread system testing of the dual polarization WSR-88D IOC is scheduled to begin in October 2009, beta testing in June 2010, and full scale deployment in October 2010. The NWS OST is managing a contract to develop and deploy the RDA hardware and software upgrade. The RPG portion of the program is being developed as a collaborative effort primarily between the NOAA's NWS OST, OHD, and ROC, and NOAA OAR NSSL, but also including many WSR-88D agency users and subject-matter-experts. Development and testing of AWIPS enhancements to support dual polarization is already complete and was done earlier than typical so that providing dual polarization capabilities to NWS forecasters would not be impacted by the AWIPS-II program which is scheduled to be deployed in the same timeframe. The new data and products associated with dual polarization will significantly increase communications and storage loads, which external systems and users will need to be prepared for. Ongoing research is anticipated to provide even greater capabilities and enhancements to WSR-88D following the initial deployment of dual polarization.

8. ACKNOWLEDGEMENTS

Thanks go to Ning Shen, Yukuan Song, James Ward, Cham Pham, Jihong Liu, and Zhan J Zhang for their help implementing the operational MLDA, HCA and QPE algorithms; and to Jim Ramer, Joanne Edwards, Xiangbao Jing, and Zihou Wang for developing, testing, and refining AWIPS software to support dual polarization product displays.

9. REFERENCES

Boodoo, S., D. Hudak, M. Leduc, and N. Donaldson, 2008: Observations of the melting layer in southern Canada with a C-band dual polarized radar. Extended Abstracts, 5th *European Conf. on Radar Meteor.*, Helsinki, Finland, 12.5. [Available online at http://erad2008.fmi.fi/proceedings/extended/erad2008-0205-extended.pdf]

Brandes, E.A., and K. Ikeda, 2004: Freezing-level estimation with polarimetric radar. Journal of Applied Meteorology, **43**, 1541-1553.

Brandes, E. A., 2000: Dual-polarization radar fundamentals and algorithm prospects, *Report on Next Generation Weather Radar Program – Operational Support Facility, WSR-88D Commerce-Defense-Transportation, May 2000*.

Doviak, R. J., V. Bringi, A. Ryzhkov, A. Zahrai, and D. Zrnic, 2000: Considerations for Polarimetric Upgrades to Operational WSR-88D Radars *Journal of Atmospheric and Oceanic Technology* **17**, 257–278.

Giangrande, S.E., J.M. Krause, and A.V. Ryzhkov, 2008: Automatic designation of the melting layer with a polarimetric prototype of the WSR-88D radar. *Journal of Applied Meteorology and Climatology*, **47**, 1354 – 1364.

Giangrande, S., and A. Ryzhkov, 2008: Estimation of rainfall based on the results of polarimetric echo classification. *Journal of Applied Meteorology,* **47**, 2445 – 2462.

Giangrande, S. E., A. V. Ryzhkov, and J. Krause, 2005: Automatic detection of the melting layer with a polarimetric prototype of the WSR-88D radar. *32nd Conf. on Radar Meteor., Albuquerque, NM, Amer. Meteor. Soc.*.

Heinselman, P.L., and A.V. Ryzhkov, 2006: Validation of polarimetric hail detection. *Weather and Forecasting*, **21**, 839 – 850.

Henry, R., E. Welles, T. Hopkins, O. Brown-Leigh, A.M. Tarro, 2009: AWIPS II Overview and Status. *25th Conf on Interactive Information and Processing Systems*, Amer. Meteor. Soc., Phoenix, AZ, 8A.2.

Ivic, I. R., 2008: Detection Thresholds for Spectral Moments and Polarimetric Variables. University of Oklahoma, Dissertation for the School of Electrical and Computer Engineering.

Kitzmiller, D., D. Brewer, F. Ding, D. Miller, and D. Riley, 2007: Final Report Submitted to the Radar Operations Center, 54. pp. [Available at http://www.nws.noaa.gov/oh/hrl/papers/2007/ROC-MOU_FY2007_final_200711.pdf]

Park, H.S., A. Ryzhkov, D. Zrnic, and K.E. Kim, 2009: The hydrometeor classification algorithm for the polarimetric WSR-88D: Description and application to an MCS. Accepted by *Weather and Forecasting.*

ROC 2820003, 2009: Radar Operations Center, Build 12 (draft) Software Requirements Specification for Radar Product Generation Program. Includes requirements for the recombination algorithm which was developed by Pengfei Zhang, et al. at NSSL and is available online at http://publications.nssl.gov /wsr88d_reports/Super_Res_and_CLutterRPT2.pdf.

ROC NX-DR-03-061/02, 2009: Radar Operations Center, Build 12 (draft) Dual Polarimetric Preprocessor - Algorithm Description. Includes requirements for the Unwrapping algorithm which was developed by John Krause, et al. at NSSL.

ROC 2620002, 2009: Radar Operations Center, Build 12 (draft) Interface Control Document for RDA/RPG Interface. Includes Message 31 format.

Ryzhkov, A.V., T. J. Schuur, D.W. Burgess, S. Giangrande, and D.S. Zrnic, 2005: The Joint Polarization Experiment: Polarimetric rainfall measurements and hydrometeor classification. *Bulletin of American Meteorological Society,* **86**, 809 – 824.

Ryzhkov, A.V., S.E. Giangrande, and T.J. Schuur, 2005: Rainfall estimation with a polarimetric prototype of the WSR-88D radar. *Journal of Applied Meteorology*, **44**, 502 – 515.

Ryzhkov, A.V., and D. S. Zrnic, 1998: Discrimination between rain and snow with a polarimetric radar. *Journal of Applied Meteorology*, **37**, 1228-1240.

Scharfenberg, K.A and K. L. Manross, 26 January 2007: A product evaluation for the dual-polarimetric WSR-88D. *White paper for the University of Oklahoma Cooperative Institute for Mesoscale Meteorological Studies*.

Scharfenberg, K., K. Elmore, E. Foren, V. Melnikov, D.S. Zrnic, 2005: Estimating the Impact of a 3-dB Sensitivity Loss on WSR-88D Data. *32nd Conf. on Radar Meteor., Albuquerque, NM, Amer. Meteor. Soc., P12R.9.*

Scharfenberg, K., D. Miller, T. Schuur, P. Schlatter, S. Giangrande, V. Melnikov, D. Burgess, D. Andra, M. Foster, and J. Krause, 2005: The Joint Polarization Experiment: polarimetric radar in forecasting and warning decision making. *Weather and Forecasting,* **20**, 775 – 788.